

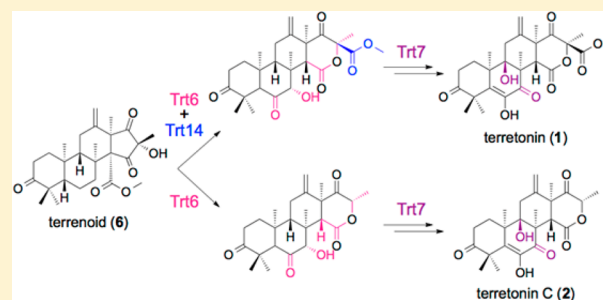
Uncovering the Unusual D-Ring Construction in Terretonin Biosynthesis by Collaboration of a Multifunctional Cytochrome P450 and a Unique Isomerase

Yudai Matsuda,[†] Taiki Iwabuchi,[†] Toshiyuki Wakimoto, Takayoshi Awakawa, and Ikuro Abe*

Graduate School of Pharmaceutical Sciences, The University of Tokyo, 7-3-1 Hongo, Bunkyo-ku, Tokyo 113-0033, Japan

S Supporting Information

ABSTRACT: Terretonin (**1**) is a fungal meroterpenoid isolated from *Aspergillus terreus*, and possesses a highly oxygenated and unique tetracyclic structure. Although the biosynthetic gene cluster for **1** has been identified and the biosynthesis has recently been studied by heterologous reconstitution and targeted-gene deletion experiments, the last few steps of the terretonin pathway after terrenoid (**6**) have yet to be elucidated. Notably, the mechanism for the D-ring expansion to afford the terretonin scaffold has been a long-standing mystery to solve. Here we report the characterization of three enzymes that convert **6** into **1**, as well as the complete biosynthetic pathway of **1**. In the proposed terretonin pathway, the cytochrome P450 Trt6 catalyzes three successive oxidations to transform **6** into an unstable intermediate, which then undergoes the D-ring expansion and unusual rearrangement of the methoxy group to afford the core skeleton of **1**. This unprecedented rearrangement is catalyzed by a novel isomerase Trt14. Finally, the nonheme iron-dependent dioxygenase Trt7 accomplishes the last two oxidation reactions steps to complete the biosynthesis.



INTRODUCTION

Structural diversity and complex molecular architectures are the key features of natural products, and therefore they exhibit a remarkably wide range of biological activities. The biosynthesis of natural products with unusual carbon skeletons should involve fascinating chemical transformations catalyzed by the responsible enzymes. The identification and characterization of these intriguing enzymes not only are interesting in terms of fundamental sciences, but also will have a significant impact on synthetic chemistry, since they might serve as efficient catalysts for difficult syntheses involving multistep chemical reactions. Thus, the biosyntheses of complex natural products have recently been studied intensively, revealing many enzymes that catalyze unprecedented chemical conversions and new families of enzymes.^{1–3} It is noteworthy that “unusual” reactions are often mediated by “usual” enzymes that share relatively high sequence similarity with well-characterized enzymes. For example, atypical reactions have recently been reported to be catalyzed by common oxidative enzymes such as cytochrome P450s,^{4–6} flavin adenine dinucleotide (FAD)-dependent enzymes,^{6–8} and nonheme and α -ketoglutarate (α -KG)-dependent dioxygenases.^{9–11} This implies that the peculiarity of the substrate is also a key factor for unique reactions to occur. However, completely new families of enzymes can also be discovered through biosynthetic analyses. For example, recent studies revealed the presence of the novel membrane-bound terpene cyclases in the pyripyropene A pathway,¹² the spiroacetal-forming enzymes in reveromycin¹³ or avermectin¹⁴ biosynthesis, the β -branching domain in rhizoxin biosyn-

thesis,¹⁵ and the enzyme for [4 + 2]-cycloaddition in the versipelostatin pathway.¹⁶ Once a new enzyme class has been identified and characterized, it considerably accelerates the functional analyses of homologous proteins that can easily be found in the public database.

Terretonin (**1**),¹⁷ isolated from *Aspergillus terreus*, is one of the fungal meroterpenoids derived from 3,5-dimethylorsellinic acid (DMOA) and farnesyl pyrophosphate (FPP), and possesses a unique tetracyclic core skeleton (Figure 1A). In the 1980s, intensive incorporation experiments using radioactive/stable isotopes were performed by Simpson's and Vederas' groups, to elucidate the biosynthetic pathway of **1** and the mechanism underlying the construction of its D-ring.^{18–21} Isotope-feeding studies suggested the following mechanism for D-ring generation as Figure 1B: after the formation of the hydroxydiketone intermediate, the intramolecular tandem lactonization and retro-Claisen cleavage would give a ring-expanded β -keto acid, which subsequently undergoes methyl esterification to afford the scaffold of **1**.

The biosynthetic gene cluster (~27.3 kb, 10 genes) for **1** (the *trt* cluster, Supporting Information Figure S1) has been identified, and heterologous expression and gene deletion studies have been performed to establish the biosynthetic pathway of **1** and its analogue terretonin C (**2**), lacking the methyl ester group at C-16.^{22–24} At present, the first seven steps in the terretonin pathway are well understood, in which

Received: January 18, 2015

Published: February 11, 2015

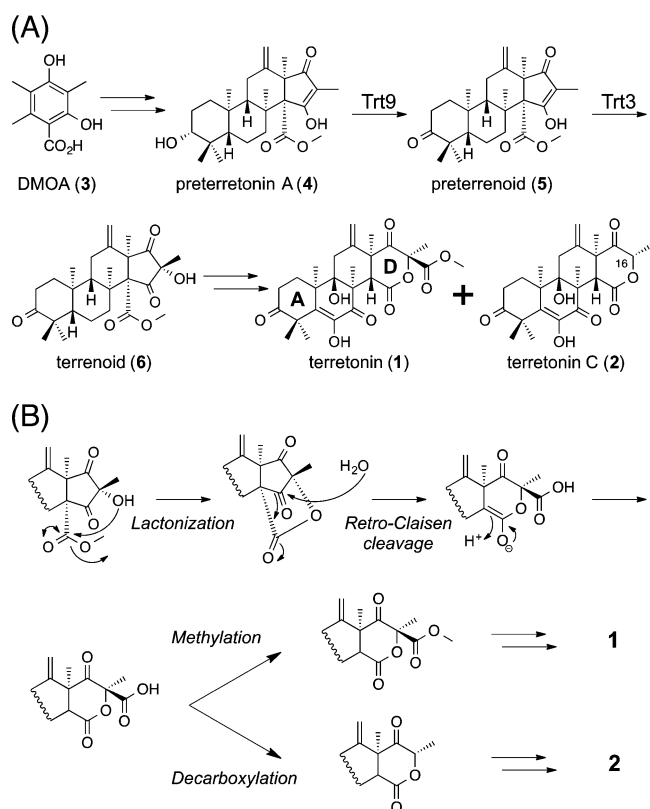


Figure 1. (A) Biosynthetic pathway of terrenoid (6). (B) Proposed reaction mechanism for the D-ring construction.

the nonreducing polyketide synthase Trt4 synthesizes DMOA (3) as the initial precursor.²² Reconstitution experiments revealed that five enzymes, including Trt4, are responsible for the generation of the first tetracyclic intermediate preterretonin A (4).²³ On the basis of the targeted-gene deletion experiments by Wang's group, 4 would then be oxidized into preterrenoid (5) by the short-chain dehydrogenase Trt9, followed by C-16 hydroxylation catalyzed by the FAD-dependent monooxygenase Trt3 to yield terrenoid (6) (Figure 1A).²⁴ Terrenoid (6) was accumulated upon the disruption of *trt6*, a cytochrome P450 monooxygenase gene, but the product(s) of Trt6 has yet to be identified. Additionally, no intermediate accumulated with the deletion of *trt7*, encoding an Fe(II) and α -KG-dependent dioxygenase, and therefore the function of Trt7 still remains unclear. Interestingly, the *trt14*-deletion mutant only produced 2 but not 1, indicating that Trt14, which shares almost no sequence homology with any characterized enzymes, is somehow involved in the formation of the methyl ester group of 1. Since 2 appears to be derived from the decarboxylation of the β -keto acid shown in Figure 1B, Trt14 was proposed to be engaged in the conversion of the β -keto acid into its methyl ester.²⁴ On the other hand, AusJ and AusH, two homologous proteins to Trt14 involved in austinol biosynthesis, are most likely to be isomerases, based on gene disruption experiments,²⁵ but they have not been studied at the enzymological level. Thus, the functional characterization of Trt14 would lead to the discovery of novel enzymatic mechanisms and facilitate studies of other homologous proteins.

In this study, we sought to elucidate the complete biosynthetic pathway of terretinin (1) and the mechanism for the D-ring construction of 1. We have determined that three

enzymes with uncharacterized functions, the cytochrome P450 Trt6, the nonheme iron-dependent dioxygenase Trt7, and the isomerase Trt14, are responsible for the conversion of 6 into 1, by in vivo and in vitro reconstitutions of the terretinin pathway. In the course of our study, we have successfully reconstructed the biosynthesis of 1 in a single heterologous host and established the biosynthetic route leading to 1, in which Trt6 performs three successive oxidative reactions, Trt14 catalyzes an unprecedented rearrangement to generate the terretinin scaffold, and Trt7 further oxidizes the B-ring to complete the biosynthesis.

RESULTS

Reconstitution of Terrenoid Biosynthesis. Although the previous gene deletion study indicated that terrenoid (6) is synthesized from preterretonin A (4) by Trt9 and Trt3,²⁴ a heterologous expression system with these two enzymes has not been constructed. To further validate the pathway leading to 6, and to provide the platform to analyze the other terretinin biosynthetic genes, we first introduced *trt9* and *trt3* into the *Aspergillus oryzae* NSAR1²⁶ transformant synthesizing 4, which we constructed previously.²³ In the expression system, the sequence of *trt9* was manually revised by comparisons with the sequences of other homologous genes such as *adrF* in the andrastin A pathway²⁷ (Figure S2). When the SDR gene *trt9* was introduced, the transformant produced the new product 5, which was not found in the control strain with the five enzymes (Figure 2A, lanes i and ii). As expected, ¹H and ¹³C NMR and

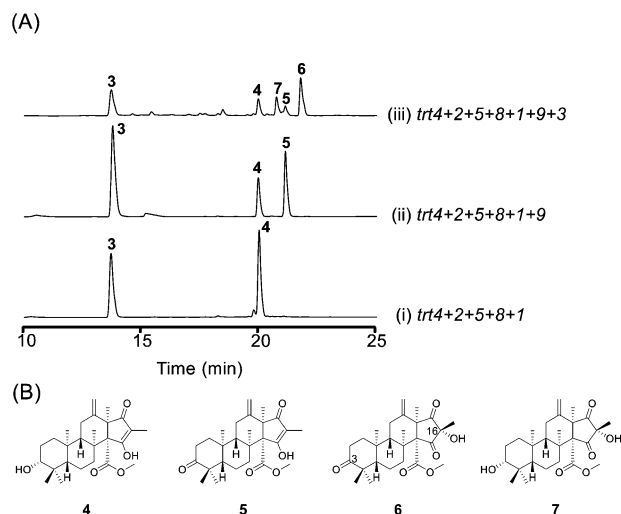


Figure 2. Reconstitution of the early stages of 1 biosynthesis in the *A. oryzae* expression system. (A) HPLC profiles of mycelial extracts from transformants harboring (i) *trt4+2+5+8+1*; (ii) *trt4+2+5+8+1+9*; (iii) *trt4+2+5+8+1+9+3*. (B) Structures of compounds 4–7. Chromatograms were monitored at 254 nm.

MS analyses revealed that the new product is preterrenoid (5), confirming the role of Trt9 as the alcohol dehydrogenase that utilizes 4 as a substrate. Further introduction of the FMO gene *trt3* successfully yielded terrenoid (6), which was absent in the six gene-expression system (Figure 2A, lane iii). The transformant also produced one minor metabolite 7, with a 2 Da larger molecular weight than that of 6. After the isolation and spectroscopic analyses, 7 was determined to be the reduced form of 6 with a secondary alcohol at the C-3 position, and was named terrenoidol (Figure 2B). Terrenoidol is most likely

generated via the direct oxidation of **4**, instead of **5**, by Trt3. Thus, it was confirmed that Trt3 is the C-16 hydroxylase.

Functional Analysis of the Cytochrome P450 Trt6.

Next, we investigated the function of the cytochrome P450 monooxygenase Trt6, which is considered to accept **6** as its substrate. The *trt6* gene was coexpressed with the other seven genes responsible for the biosynthesis of **6**, and the LC-MS analyses of the resulting metabolites clearly revealed the presence of two new compounds, **8** and **9** with m/z 417 $[M + H]^+$ and 419 $[M + H]^+$, respectively (Figure 3A, lanes i and

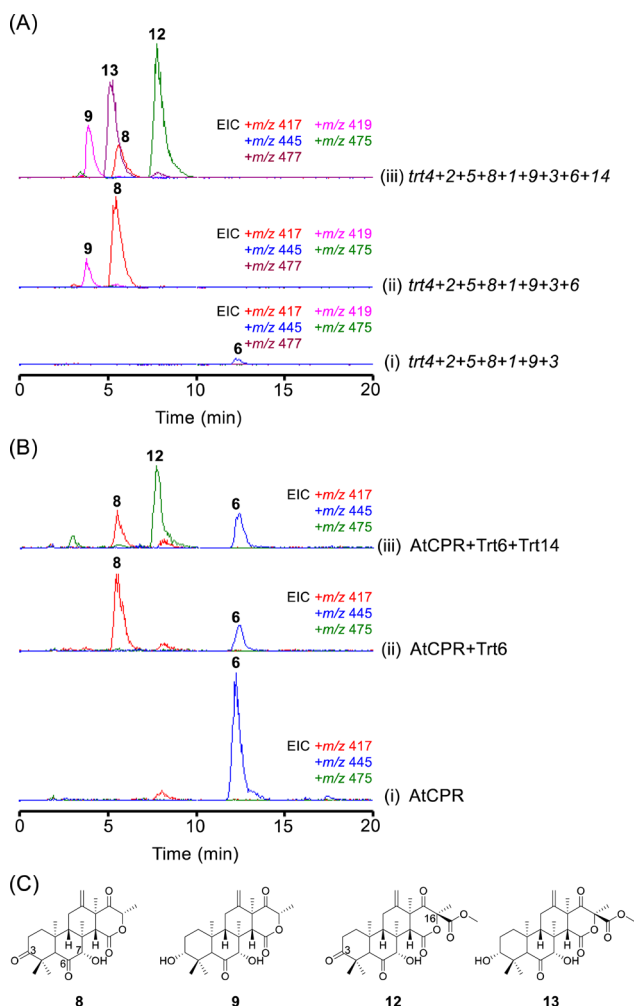


Figure 3. Functional analyses of Trt6 and Trt14. (A) LC-MS profiles of culture supernatant extracts from *A. oryzae* transformants harboring (i) *trt4+2+5+8+1+9+3*; (ii) *trt4+2+5+8+1+9+3+6*; (iii) *trt4+2+5+8+1+9+3+6+14*. (B) LC-MS profiles of the products from in vitro enzymatic reactions of Trt6 and Trt14 with **6**: (i) reaction with only AtCPR; (ii) reaction with AtCPR and Trt6; (iii) reaction with AtCPR, Trt6, and Trt14. (C) Structures of compounds **8**, **9**, **12**, and **13**.

ii). The molecular formula of **8** was established by high-resolution MS analysis to be $C_{24}H_{32}O_6$, which is consistent with the presence of only 24 signals in the ^{13}C NMR spectrum. Thus, two carbon atoms were somehow lost during the formation of **8**. Interestingly, the 1H NMR spectra of **8** were quite different from those of **6**, in which the signal for the methyl ester disappeared, and one methyl signal at δ_H 1.46, coupled with a methine newly appearing at δ_H 5.04, was detected as a doublet ($J = 6.2$ Hz). Collectively, it was

suggested that the D-ring expansion followed by the decarboxylation, as shown in Figure 1, occurred to generate **8**. As the proposed mechanism for the ring expansion results in the loss of two oxygen atoms, two additional oxygen atoms should be introduced upon the formation of **8**. Further interpretation of the one- and two-dimensional (2D) NMR spectra confirmed the existence of a ketone at C-6 and an α -hydroxyl group at C-7 as well as the complete structure of **8**, which was named terretonin H (Figure 3C). Product **9**, designated as terretonin I, was characterized as the reduced form of **8** with a C-3 hydroxyl group (Figure 3C), and appears to be derived from **7**. Thus, the results indicated that Trt6 not only is involved in the three successive oxidations on the B-ring of **6** or **7** but also causes the expansion of the D-ring to afford the scaffold of terretonin C (**2**). Given that the proposed mechanism for the ring expansion is not a typical oxygenase-catalyzed reaction, Trt6 could only catalyze the B-ring oxidation, and the D-ring rearrangement could be a fortuitous result due to the conformational change induced by the functional groups introduced to the B-ring.

To obtain further insight into the Trt6-catalyzed reaction, a microsomal fraction of an *A. oryzae* transformant harboring *trt6* and the cytochrome P450 reductase gene from *A. terreus* (AtCPR)²⁸ was prepared and subjected to an in vitro assay. The reaction was performed with **6** as the substrate and NADPH, and was analyzed by LC-MS, which confirmed the production of **8** only in the presence of Trt6 (Figure 3B, lanes i and ii, Figure S3).

Terretonin C Biosynthesis with the Dioxygenase Trt7.

The Trt6-derived product, **8**, possesses the same carbon skeleton as that of terretonin C (**2**), and **8** should undergo two rounds of oxidation to yield **2**. Thus, we reasoned that Trt7, which is a putative Fe(II)/ α -KG-dependent dioxygenase with an uncharacterized function encoded by the *trt* cluster, converts **8** into **2**, in a similar manner to the other multifunctional dioxygenases, AusE and AndA, found in the fungal meroterpenoid pathways.^{9,10} To investigate this hypothesis, *trt7* was expressed in *A. oryzae* along with the eight other genes involved in the formation of **8**. The culture supernatant extract was analyzed by HPLC and LC-MS, and the major metabolite **2** and the minor product **10** were observed by the addition of *trt7* (Figure 4A, lanes i and ii). After isolation and NMR/MS analyses, **2** was identified as terretonin C, as expected. On the other hand, **10**, with a molecular weight 16 Da less than that of **2**, was later isolated from the ten gene-expressing transformant (Figure 4A, lane iii). Product **10**, designated as terretonin J, was then determined to be the biosynthetic precursor of **2** lacking the hydroxyl group at the C-9 position. Taken together, Trt7 is responsible for the last two steps in terretonin C biosynthesis, by catalyzing the oxidations at both C-7 and C-9.

Functional Characterization of Trt14. As the previous study indicated,²⁴ we were unable to obtain terretonin (**1**) or its analogues with a methyl ester group at C-16 in the absence of Trt14, which shares almost no amino acid sequence homology with characterized proteins. To investigate whether Trt14 is indeed engaged in the formation of the methyl ester embedded in the structure of **1**, we constructed a heterologous expression system with all ten of the genes in the *trt* cluster, including *trt14*, and analyzed its metabolites. As a result, the transformant successfully produced **1** and its precursor terretonin A (**11**)²⁹ which were not detected in the nine gene-expression system without *trt14*, and also yielded a significant amount of **2** as well (Figure 4A, lane iii). Thus, Trt14 actually plays a role in the

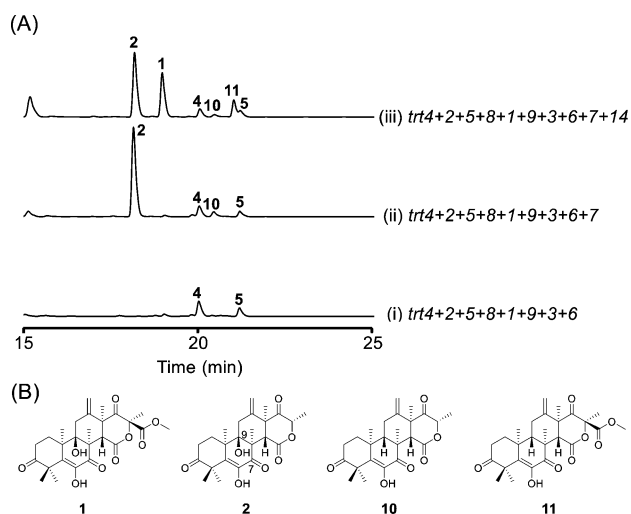


Figure 4. Functional analysis of Trt7 and complete heterologous reconstitution of the terretinin biosynthesis. (A) HPLC profiles of culture supernatant extracts from *A. oryzae* transformants harboring (i) *trt4+2+5+8+1+9+3+6*; (ii) *trt4+2+5+8+1+9+3+6+7*; (iii) *trt4+2+5+8+1+9+3+6+7+14*. (B) Structures of compounds **1**, **2**, **10**, and **11**. Chromatograms were monitored at 277 nm.

methyl ester formation, and we have successfully established the minimum gene set required for terretinin biosynthesis by reconstitution experiments.

Given the production of **1**, the question now arises about the catalytic role of Trt14 in the terretinin pathway. Since it is unlikely that **2** is the precursor of **1**, one reasonable explanation is that Trt14 methylates the carboxyl group of the Trt6-derived intermediate before the decarboxylation occurs. However, considering the fact that Trt14 shares no homology with known methyltransferases, and that AusJ and AusH, the two homologues of Trt14 involved in the austinol pathway,²⁵ seem to be isomerases, it is unlikely that Trt14 acts as a methyltransferase. Hence, this led us to hypothesize that the methyl ester is formed via an intramolecular rearrangement of the methoxy group that is originally bound to C-25 of **6**. To clarify the origin of the methyl group of the methyl ester, we performed an isotope-incorporation experiment with [methyl-¹³C]methionine, which was added to the growth medium for the *A. oryzae* strain synthesizing **4**. The resultant metabolite is labeled with ¹³C at the C-22, -24, and -1' positions (Figure S32), and this labeled **4** was further incubated with a transformant expressing *trt9*, 3, 6, 7, and 14 to yield ¹³C-labeled terretinin (**1**). Assuming that Trt14 works as a methyltransferase, C-1' of **1** should be unlabeled, while the position would become labeled upon the intramolecular rearrangement. The ¹³C NMR spectrum of the metabolite clearly revealed the labeling of the molecule at three positions, including C-1' (Figures 5 and S33), thus excluding the proposal that Trt14 is a methyltransferase and supporting the involvement of the intramolecular transfer of the methoxy group.

To obtain Trt14-derived metabolite(s) and to establish the complete biosynthetic pathway to **1**, we constructed a transformant expressing *trt14* as well as the eight genes for the generation of **8**. As expected, the transformant produced two new metabolites, **12** and **13** with *m/z* 475 [M + H]⁺ and 477 [M + H]⁺, respectively (Figure 3A, lane iii). Product **12**, which was identified as terretinin D,²⁹ possesses a similar structure to that of **8** but additionally contains a methyl ester

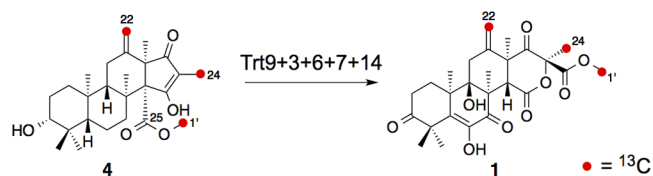


Figure 5. Labeling experiment using [methyl-¹³C]methionine.

group at the C-16 position, corroborating the role of Trt14 as the methyl ester-forming enzyme. As in the cases of **7** and **9**, product **13**, which is designated as terretinin K, was found to have the same carbon skeleton as that of **12**, and only differs at C-3 with a hydroxyl functionality. Thus, **12** would be the key intermediate of the terretinin pathway that lies between terrenoid (**6**) and terretinin A (**11**).

Next, we sought to characterize Trt14 by in vitro assays using recombinant Trt14 heterologously expressed in *Escherichia coli*. The purified Trt14 was incubated with the microsomal fraction containing Trt6 and AtCPR, in the presence of **6** as the substrate. The reaction extract was subjected to LC-MS analysis, which revealed the production of **12** in a Trt14-dependent manner (Figure 3B, lane iii, Figure S4). No additional cofactors or metals were required for the activity of Trt14. This result clearly demonstrates that Trt14 works collaboratively with the P450 monooxygenase Trt6 to generate the terretinin scaffold.

We also performed the reaction with only Trt14 and the substrate **6**, which yielded the isomerized product **14** (Figure 6A). After the preparative-scale enzymatic reaction, **14** was

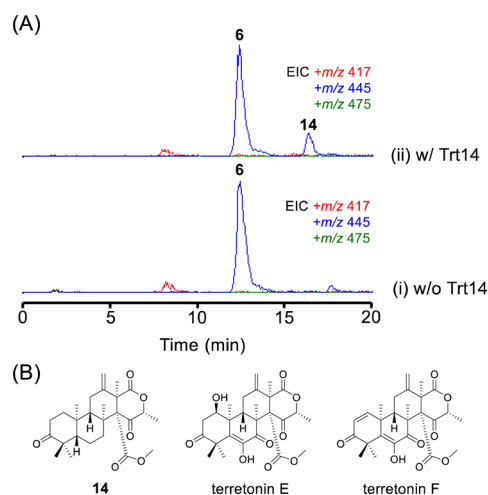
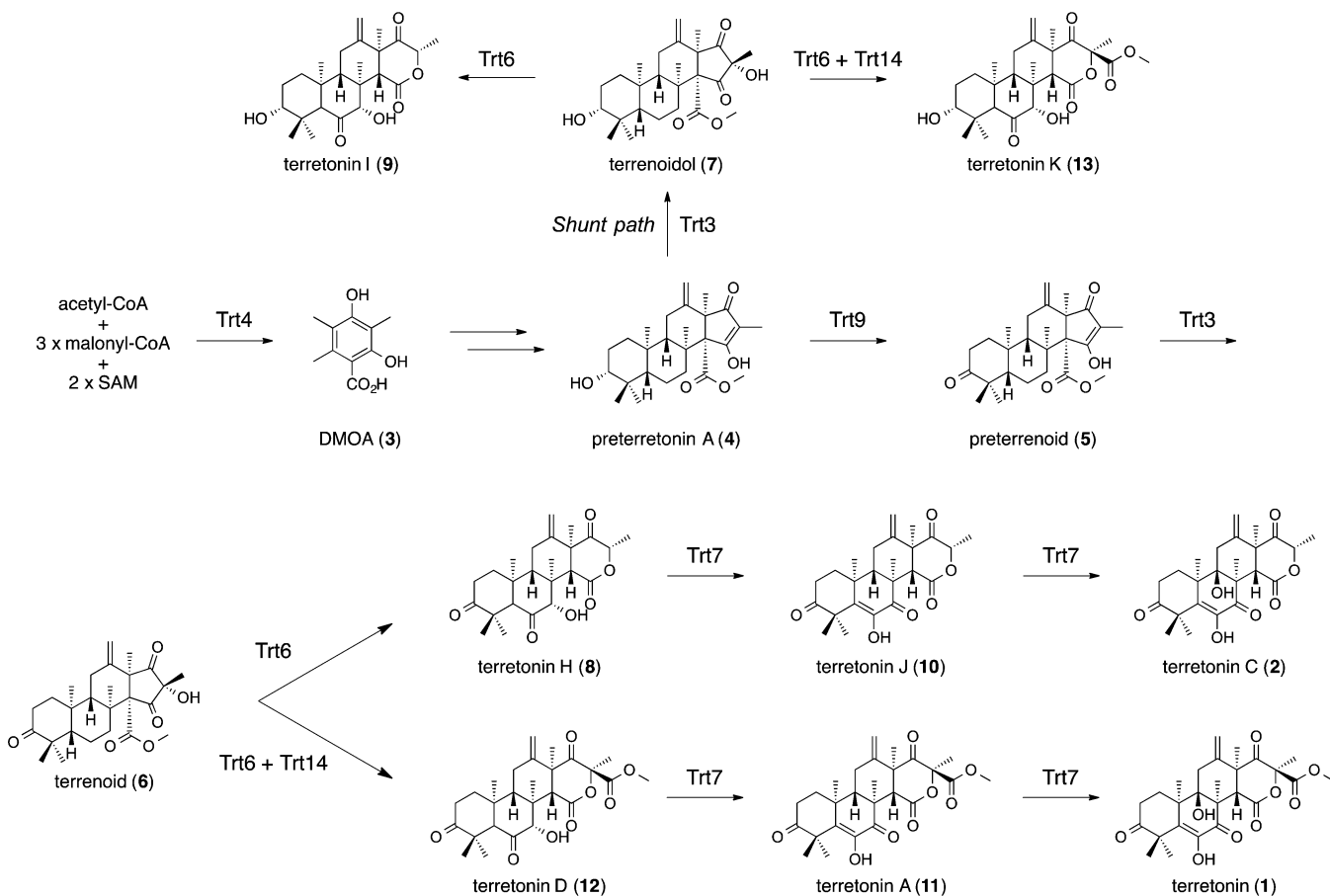


Figure 6. LC-MS profiles of the products from in vitro enzymatic reactions of Trt14 with **6**: (i) without Trt14; (ii) with 15 μ M of Trt14. (B) Structures of **14**, terretinin E, and terretinin F.

isolated and subjected to NMR analyses. The ¹H NMR spectrum of **14** is somewhat similar to that of **6**, but revealed one additional methine signal at δ_H 5.01 (q, *J* = 6.2 Hz) coupled with a methyl signal at δ_H 1.41. In the ¹³C NMR spectrum, one signal around δ_C 210 disappeared, and alternatively, a new signal appeared at δ_C 171.9, which is indicative of the emergence of an ester group. Taken together, we thought that the δ -lactone D-ring present in **1** was generated. Very surprisingly, further analyses by 2D NMR spectra, however, revealed that the methyl ester group is retained at C-14, and that the positions of the ester and α -methyl ketone of the D-

Scheme 1. Complete Biosynthetic Pathway of Terretonin (1)



ring are reversed from those of **1**. Interestingly, **14**, which we named terretonin L, has the same carbon skeleton as those of terretonin E and terretonin F^{30,31} (Figure 6B). Given that the intramolecular rearrangement of the methyl ester was not observed when **6** was utilized as the substrate, the functional groups on the B-ring could play a crucial role in the drastic conversion to afford the terretonin scaffold.

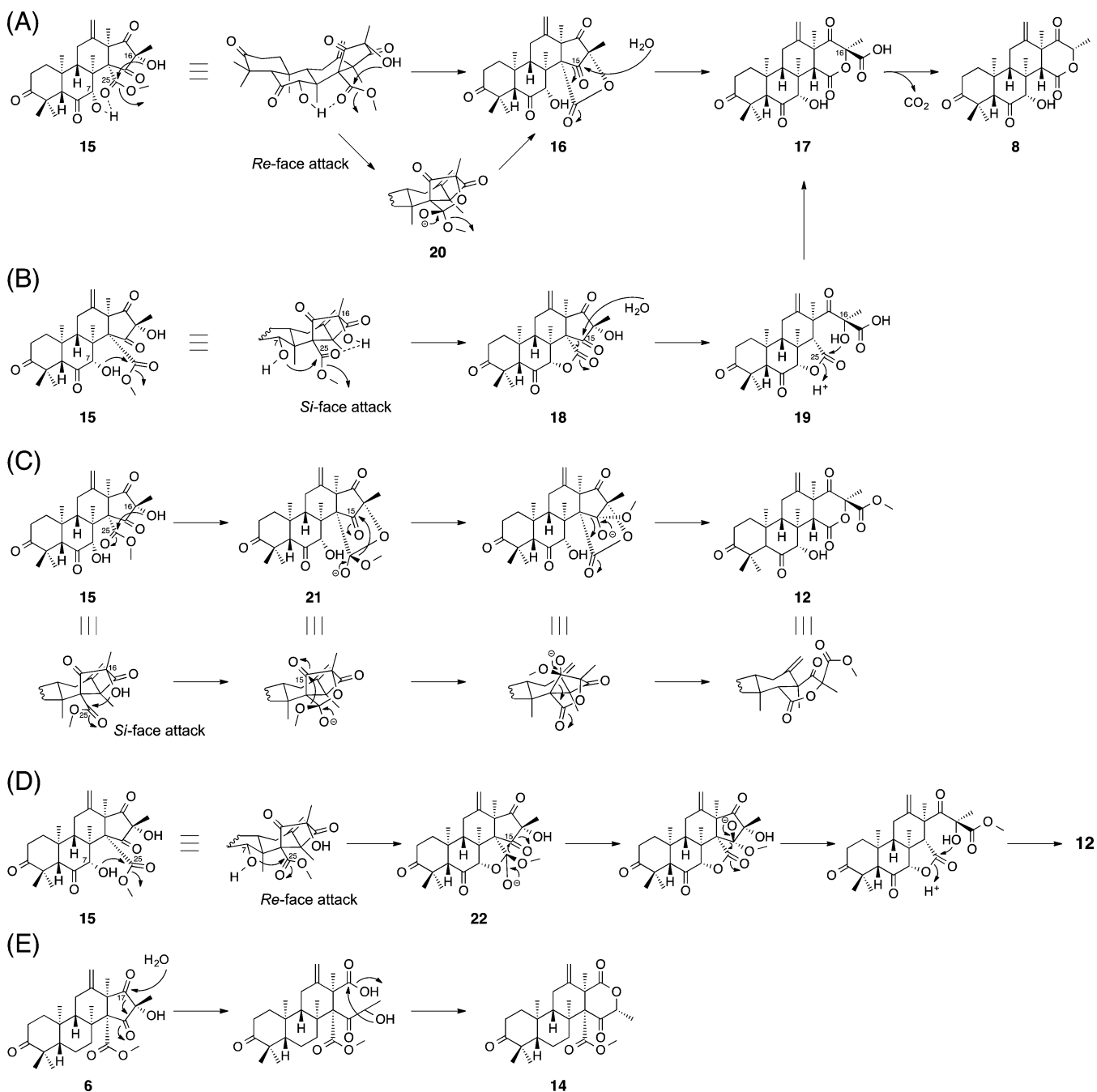
DISCUSSION

In this study, we have successfully established the complete biosynthetic pathway leading to terretonin (**1**) and terretonin C (**2**) by characterizing the functions of three enzymes, Trt6, Trt7, and Trt14, and by isolating key intermediates including previously undescribed molecules (Scheme 1). Targeted-gene deletion experiments are a powerful tool for the functional prediction of biosynthetic genes. However, the complete determination of the pathway is sometimes hampered by the lack of intermediate accumulation upon gene deletion; indeed several key intermediates such as **8**, **10**, **11**, and **12** were not obtained in the gene disruption experiment.²⁴ As we have demonstrated in this study, as well as in our previous study on anditomin,¹⁰ multiple genes (~10 genes) can now be readily introduced into *A. oryzae* heterologous expression system, and the resulting metabolites are usually obtainable in good yield. Remarkably, the yield of **2** reached ~60 mg/L even after the introduction of nine biosynthetic genes. Collectively, the combination of targeted-gene deletion and heterologous fungal expression will further accelerate biosynthetic studies on fungal natural products.

The terretonin pathway requires 10 dedicated enzymes, which is fewer than the sum predicted based on the number of reactions required for the biosynthesis. This is mainly attributed to the involvement of two multifunctional oxygenases; the P450 monooxygenase Trt6 and the nonheme iron-dependent dioxygenase Trt7 are responsible for three and two successive oxidation reactions, respectively. Multiple oxidation and structural complexification by a single enzyme have recently been reported for many fungal natural products, as exemplified by the P450s in the lovastatin,²⁸ fumagillin,⁵ and andrastin A²⁷ biosyntheses, the α -KG-dependent dioxygenases in the austinol,⁹ anditomin,¹⁰ and viridicatin¹¹ biosyntheses, and the FAD-dependent monooxygenase in cytochalasin E biosynthesis.⁷ Thus, oxidative enzymes in natural product biosyntheses significantly contribute to the structural diversification and complexification. Further exploration of the oxygenases will indeed lead to the discovery of other intriguing enzymatic transformations.

One of the key reactions in the terretonin pathway is the D-ring construction, and the underlying mechanism has been a long-standing question. Although we were unable to isolate any intermediates between terretonidol (**6**) and terretonin H (**8**), the mechanisms for this rearrangement could be proposed as follows. Considering that Trt6, the key enzyme for the ring expansion, is a P450 monooxygenase, it is unlikely that the rearrangement is catalyzed by an oxidative enzyme. Since **6** does not undergo spontaneous ring expansion, it is most likely that the functional oxygen groups on the B-ring introduced by Trt6 would have some effect on the D-ring expansion.

Scheme 2. Proposed Reaction Mechanisms for the Transformations (A, B) Mediated by Trt6 and (C–E) Catalyzed by Trt14



Additionally, as the ring expansion causes the huge structural change, it is most likely that Trt6 oxidizes **6** in a successive manner before the rearrangement occurs, and that the P450 yields **15**, which is the analogue of **6** with the oxidized B-ring (Scheme 2A). Given that the C-7 hydroxyl group is α -oriented, it would form a hydrogen bond with the carbonyl oxygen of the methyl ester of the predicted intermediate **15** (Scheme 2A). The hydrogen bond could activate the carbonyl to induce the lactonization via the nucleophilic attack by the C-16 alcohol. The resulting intermediate **16** would then undergo retro-Claisen type cleavage at the β -ketoester moiety to yield the ring-expanded β -keto acid **17**. Spontaneous decarboxylation then converts **17** into **8**, to complete the reaction. Alternatively, the C-7 alcohol first attacks the carbonyl carbon of the methyl ester to produce the γ -lactone **18**, in which the C-25 carbonyl

oxygen could form a hydrogen bond with the C-16 hydroxyl group to accelerate the reaction as in the first proposal (Scheme 2B). The retro-Claisen reaction of **18** at C-15 would provide the ring-opened intermediate **19**, which undergoes the lactonization between the C-17 alcohol and the C-25 carbonyl to generate **17**.

Another intriguing point in the terretonin pathway is the Trt14-catalyzed methyl ester formation. Assuming that **15** undergoes the lactonization with the hydrogen bond between the C-7 alcohol and the C-25 carbonyl, as shown in Scheme 2A, the hydroxyl group should attack the *Re*-face of the carbonyl, resulting in the tetrahedral anionic intermediate **20** (Scheme 2A). Supposing the intramolecular nucleophilic attack at the C-15 ketone by the leaving methoxide ion instead of water, an analogue of **17**, but with a methyl ester group at C-16, could be

obtained. However, the direction of the methoxy group in **20** is apparently unfavorable for attacking the C-15 carbonyl carbon. In contrast, Trt14 might reverse the face selectivity to induce the *Si*-face attack, in which the resulting intermediate **21** possesses the methoxy group that is adjacent to the C-15 (Scheme 2C). In the second possible mechanism, involving the lactonization between the C-7 alcohol and the C-25 carbonyl (Scheme 2B), the generated methoxide ion would attack the C-15 to initiate the retro-Claisen reaction. As in the case of the first proposal, the C-7 alcohol would attack the *Re*-face of the C-25 carbonyl to make the methoxy group of **22** proximate to C-15 (Scheme 2D), while the hydroxyl group would attack the *Si*-face when the hydrogen bond between the C-25 carbonyl and the C-16 alcohol is formed (Scheme 2B). Taken together, Trt14 would activate the functional oxygen group(s) of the predicted substrate **15** and arrange the methoxy group of the methyl ester so that the intramolecular attack by the methoxide ion on C-15 can proceed, and/or would protect the unstable intermediate such as **21**, from water molecules to make the methoxide ion the only nucleophile that can induce the retro-Claisen cleavage.

Although this methoxy rearrangement has not been proposed to date, the reaction is consistent with the previous isotope feeding experiment by Simpson's and Vederas' groups (Figure S5).²⁰ In their incorporation study, ethyl DMOA doubly labeled with ¹⁸O and ¹³C at either the C-2 alcohol or the C-7 carbonyl was used in an equal amount. The labeled substrate is hydrolyzed into DMOA (**3**) before incorporation into the terretionin pathway, and therefore the two oxygen atoms bound to C-7 of **3** are both labeled equally. The methoxy oxygen of labeled terretionin (**1**) was labeled with ¹⁸O, and this was originally attributed to the existence of a free carboxylic acid before the methyl esterification occurs. However, this position should also be labeled upon the methoxy rearrangement, supporting our proposed mechanisms.

Trt14 also catalyzes another rearrangement, in which terretionin L (**14**) is synthesized from terrenoid (**6**). The reaction would be initiated by the nucleophilic attack of water at the C-17 ketone to yield the ring-opened intermediate, which could be followed by the lactonization to generate **14** (Scheme 2E). In this conversion, Trt14 would probably activate the C-17 carbonyl and/or water molecule to perform the β -diketone cleavage. Given that **14** has the scaffold of terretionin E and terretionin F^{30,31} and that no molecule with the same carbon skeleton as **14** could be obtained in the coupling reaction with the P450 Trt6, the biosynthesis of terretionin E and terretionin F should involve an enzyme that is similar to Trt14 but is functionally specialized for the ring expansion reaction. Furthermore, the observation that the methoxy rearrangement could not be detected without the oxygenated functional groups on the B-ring suggests that the C-7 alcohol functionality is essential for the rearrangement. Thus, the mechanism described in Scheme 2D is more likely, but further work including X-ray crystallography is required to fully elucidate the reaction mechanism.

Interestingly, a homology search of Trt14 using the Phyre2³² server suggested that Trt14 is structurally similar to proteins such as ketosteroid isomerase,³³ limonene-1,2-epoxide hydrolase,³⁴ the polyketide cyclase SnoaL,³⁵ and the epoxide hydrolase MonBl,³⁶ although their sequences share almost no homology with that of Trt14. Like Trt14, these enzymes are all small proteins that consist of less than 150 amino acid residues, and additionally, aspartate residues are thought to be

catalytically important in all four enzymes. A sequence comparison of Trt14 with its homologous enzymes such as AusJ, AusH, and AusF involved in the austinol pathway,²⁵ revealed several highly conserved aspartate residues as well as glutamates (Figure S6). Considering the structural and reaction similarities between Trt14 and the above-mentioned enzymes, these conserved acidic residues could play a central role in the Trt14-catalyzed reaction. On the other hand, despite the analogy in the reactions, Trt14 exhibits no apparent similarity with the known β -diketone hydrolases, such as the 6-oxo camphor hydrolase³⁷ and the oxidized polyvinyl alcohol hydrolase,³⁸ in either primary or secondary structures.

CONCLUSION

The mechanism of D-ring construction in terretionin biosynthesis has been a long-standing mystery since the isolation in 1979. In this study, we answered this question by identifying all of the dedicated enzymes in the terretionin pathway. We have established the complete biosynthetic pathway of terretionin, and identified Trt14 as a new type of isomerase that is engaged in the highly unique rearrangement. Two multifunctional oxygenases, the cytochrome P450 Trt6 and the nonheme iron-dependent dioxygenase Trt7, are also key components in terretionin biosynthesis, thus providing another example in which an oxidative enzyme is responsible for drastic structural rearrangement and diversification. However, further investigation on the multifunctional P450 Trt6 and the unique isomerase Trt14, including mutagenesis and X-ray crystallography, should be performed to conclusively solve the problem, and are now in progress in our laboratory.

MATERIALS AND METHODS

Strains and Media. *Aspergillus terreus* NIH 2624 was cultivated at 30 °C, 160 rpm in DPY medium (2% dextrin, 1% hipolypepton (Nihon Pharmaceutical Co., Ltd.), 0.5% yeast extract (Difco), 0.5% KH₂PO₄, and 0.05% MgSO₄·7H₂O) for 3 days, and used as the source for the cloning of each gene in the *trt* cluster as well as the *AtCPR* gene.

Aspergillus oryzae NSAR1 (*niaD*⁻, *sC*⁻, Δ *argB*, *adeA*⁻)²⁶ was used as the host for fungal expression. Transformants of the *A. oryzae* strain were grown in shaking cultures in DPY medium for 6 days, at 30 °C and 160 rpm. The cells were then transferred into Czapek-Dox (CD) medium with hipolypepton (10 g/L), and starch (20 g/L) to induce expression under the α -amylase promoter, and the cultures were shaken for three to 6 days further.

Standard DNA engineering experiments were performed using *Escherichia coli* DH5 α , purchased from Clontech (Mountain View, CA). *E. coli* cells carrying each plasmid were grown in Luria–Bertani medium and were selected with appropriate antibiotics. *E. coli* Rosetta2(DE3) (Novagen) was used for the expression of Trt14.

Construction of Fungal Expression Plasmids. For the construction of one-gene containing fungal expression plasmids, each gene in the *trt* cluster was amplified from *A. terreus* NIH 2624 genomic DNA, with the primers listed in Tables S1 and S2. The full-length *trt* genes were purified, digested with appropriate restriction enzymes, if necessary, and ligated into the pTAex3,³⁹ pUSA,⁴⁰ or pUNA⁴¹ vectors using an In-Fusion HD Cloning Kit or Ligation Kit Ver. 2.1 (TaKaRa) according to the manufacturer's protocol (Table S2). For introduction into pAdeA⁴² and pBARI,¹⁰ a fragment containing the *amyB* promoter (*PamyB*) and the *amyB* terminator (*TamyB*) was amplified from the pTAex3-based plasmids, and ligated into each vector (Table S2).

Transformation of *Aspergillus oryzae* NSAR1. Transformation of *A. oryzae* NSAR1 was performed by the protoplast–polyethylene glycol method reported previously.⁴³ The previously constructed transformant coexpressing *trt4*, *trt2*, *trt5*, *trt8*, and *trt1* was transformed with pUNA-trt9+3 to construct the seven gene-expression system, and

was further transformed with pBARI-trt6+7+14 to generate the 10 gene-expressing strain.²² When constructing the transformants with *trt9*, *trt3*, *trt6*, *trt14*, and *trt7*, two plasmids, pUNA-trt9+3 and pBARI-trt6+7+14, were used to transform *A. oryzae* NSAR1. To construct the coexpression system of Trt6 and AtCPR, pAdeA-trt6 and pUSA-AtCPR were used to transform *A. oryzae* NSAR1. For the construction of negative control strains that do not express one or more genes, the corresponding void vectors or plasmids with only one gene were used for the transformation.

HPLC Analysis of Each Product. Products from each of the transformants were analyzed by HPLC, with a solvent system of 0.5% acetic acid (solvent A) and acetonitrile containing 0.5% acetic acid (solvent B), at a flow rate of 1.0 mL/min and a column temperature of 40 °C. Separation was performed with solvent B/solvent A (20:80) for 5 min, a linear gradient from 20:80 to 100:0 within the following 20 min, 100:0 for 5 additional min, and a linear gradient from 100:0 to 20:80 within the following 3 min.

LC-MS Analysis of Each Product. Products from each of the transformants and the in vitro reaction mixture were analyzed by LC-MS, with a solvent system of 1.0% acetic acid (solvent A) and acetonitrile containing 1.0% acetic acid (solvent B), at a flow rate of 0.2 mL/min and a column temperature of 20 °C. Separation was performed with solvent B/solvent A (50:50) for 5 min, a linear gradient from 50:50 to 75:25 within the following 15 min, and a linear gradient from 75:25 to 50:50 within the following 5 min.

Isolation and Purification of Each Metabolite. For the isolation of each metabolite, 1–4 L of the culture media were extracted with ethyl acetate. Mycelia were extracted with acetone at room temperature overnight, concentrated, and reextracted with ethyl acetate. Both extracts were combined and subjected to silica-gel column chromatography and further purification by preparative HPLC. The detailed purification procedures for each compound are described in the Supporting Information.

Expression and Enzymatic Reaction Assay of Trt6. Mycelia from a three day culture of *A. oryzae* transformed with Trt6 and AtCPR were ground in liquid nitrogen, suspended in 25 mL of the reaction buffer (50 mM HEPES pH 7.5, 1.0 mM EDTA, 20% glycerol, 1.5 mM 2-mercaptoethanol), and disrupted with a French Press (25 000 psi). After removing the cell debris by centrifugation at 5800g, ultracentrifugation was performed at 100 000g to obtain the microsomal fraction, which was then suspended in the reaction buffer.

The enzymatic reaction of Trt6 with terrenoid (6) was performed in a reaction mixture containing 193 μ L of microsomal fraction, 2.5 mM NADPH, and 0.5 mM 6, in a final volume of 200 μ L. After an incubation at 30 °C for 12 h, the reaction mixture was extracted with ethyl acetate. After evaporation, the extract was analyzed by LC-MS/MS.

Labeling Experiment of Terretinin (1). To a 500 mL DPY culture of the *A. oryzae* transformant harboring *trt4*, *trt2*, *trt5*, *trt8*, and *trt1*, 200 mg of [methyl-¹³C]methionine was added, and the culture was continued at 30 °C and 160 rpm for 4 days. The labeled preterretinin A (4) was extracted and purified (see Supporting Information for the detailed purification procedure), and then further incubated with the *A. oryzae* transformant possessing *trt9*, *trt3*, *trt6*, *trt7*, and *trt14* in a 360 mL culture, incubated at 30 °C and 160 rpm for 4 days. After isolation, the labeled terretinin (1) was analyzed by NMR.

Expression and Purification of Trt14. To express *trt14* in *E. coli*, *trt14* was introduced into the pET-28a(+) vector (Novagen). The full-length *trt14* gene was amplified with the primers listed in Tables S1 and S2, purified, digested with *Nde*I and *Xho*I, and ligated into the pET-28a(+) vector using a Ligation Kit Ver. 2.1 (Table S2).

For the expression of Trt14, *E. coli* Rosetta2(DE3) was transformed with the pET-28a(+)-*trt14* plasmid. The transformant was incubated with shaking at 37 °C/160 rpm, in LB medium supplemented with 100 mg/L kanamycin sulfate. Gene expression was induced by the addition of 0.5 mM IPTG when the cultures had grown to an OD₆₀₀ of 0.6, after which the incubation was continued for 14 h at 30 °C/160 rpm. The cells were harvested by centrifugation, resuspended in lysis buffer (50 mM Tris-HCl, pH 7.5, 150 mM NaCl, 5 mM imidazole, 5%

glycerol), and lysed on ice by sonication. The cell debris was removed by centrifugation, and the supernatant was loaded onto a Ni-NTA affinity column, which was washed with 30 column volumes of wash buffer (50 mM Tris-HCl, pH 7.5, 150 mM NaCl, 10 mM imidazole, 5% glycerol). The His-tagged protein was eluted with 5 column volumes of elution buffer (50 mM Tris-HCl, pH 7.5, 150 mM NaCl, 300 mM imidazole, 5% glycerol). The purity of the enzymes was analyzed by sodium dodecyl sulfate polyacrylamide gel electrophoresis (SDS-PAGE). The protein concentration was determined using a UV-1700 PharmaSpec Spectrophotometer (Shimadzu).

Enzymatic Reaction Assays of Trt6 and Trt14. The enzymatic reactions of Trt6 and Trt14 with terrenoid (6) were performed in reaction mixtures containing 192 μ L of microsomal fraction, 2.5 mM NADPH, 0.5 mM of 6, and 0.25 μ M of Trt14, in a final volume of 200 μ L. After an incubation at 30 °C for 12 h, the reaction mixture was extracted with ethyl acetate. After evaporation, the extract was analyzed by LC-MS/MS.

Enzymatic Reaction Assay with Only Trt14. The enzymatic reaction of Trt14 with terrenoid (6) was performed in a reaction mixtures containing 50 mM Tris-HCl (pH 7.5), 2.0 mM of 6, 150 mM NaCl, 10 mM imidazole, 5% glycerol, and 15 μ M of Trt14, in a final volume of 100 μ L. After an incubation at 30 °C for 12 h, the reaction mixture was extracted with ethyl acetate. After evaporation, the extract was analyzed by LC-MS/MS.

Preterrenoid (5). White solid; $[\alpha]_D^{22}$ –53.0 (c 1.00, CHCl₃); for UV spectrum, see Figure S7; for ¹H and ¹³C NMR data, see Table S5 and Figures S12 and S13; HR-FAB-MS found *m/z* 429.2623 [M + H]⁺ (calcd 429.2641 for C₂₆H₃₇O₅). The NMR data are in good agreement with the reported data,²⁴ but are slightly revised and updated in this study.

Terrenoid (6). Yellowish white solid; $[\alpha]_D^{22}$ –26.5 (c 1.00, CHCl₃); for UV spectrum, see Figure S7; for ¹H and ¹³C NMR data, see Table S6 and Figures S14 and S15; HR-FAB-MS found *m/z* 445.2576 [M + H]⁺ (calcd 445.2590 for C₂₆H₃₇O₆). The NMR data are in good agreement with the reported data.²⁴

Terrenoidol (7). White solid; $[\alpha]_D^{22}$ +0.5 (c 0.13, CHCl₃); for UV spectrum, see Figure S7; for ¹H and ¹³C NMR data, see Table S7 and Figures S16 and S17; HR-FAB-MS found *m/z* 447.2766 [M + H]⁺ (calcd 447.2747 for C₂₆H₃₉O₆).

Terretinin H (8). White solid; $[\alpha]_D^{22}$ –160.5 (c 1.00, CHCl₃); for UV spectrum, see Figure S7; for ¹H and ¹³C NMR data, see Table S8 and Figures S18 and S19; HR-FAB-MS found *m/z* 417.2293 [M + H]⁺ (calcd 417.2277 for C₂₄H₃₃O₆).

Terretinin I (9). Colorless solid; $[\alpha]_D^{22}$ –78.3 (c 0.48, CHCl₃); for UV spectrum, see Figure S7; for ¹H and ¹³C NMR data, see Table S9 and Figures S20 and S21; HR-FAB-MS found *m/z* 419.2439 [M + H]⁺ (calcd 419.2434 for C₂₄H₃₅O₆).

Terretinin J (10). Colorless solid; $[\alpha]_D^{22}$ –106.5 (c 0.11, CHCl₃); for UV spectrum, see Figure S7; for ¹H and ¹³C NMR data, see Table S10 and Figures S22 and S23; HR-FAB-MS found *m/z* 415.2139 [M + H]⁺ (calcd 415.2121 for C₂₄H₃₁O₆).

Terretinin A (11). White solid; $[\alpha]_D^{22}$ –111.7 (c 0.44, CHCl₃); for UV spectrum, see Figure S7; for ¹H and ¹³C NMR data, see Table S11 and Figures S24 and S25; HR-FAB-MS found *m/z* 473.2189 [M + H]⁺ (calcd 473.2175 for C₂₆H₃₃O₈). The NMR data are in good agreement with the reported data.²⁹

Terretinin D (12). Colorless solid; $[\alpha]_D^{22}$ –43.9 (c 1.00, CHCl₃); for UV spectrum, see Figure S7; for ¹H and ¹³C NMR data, see Table S12 and Figures S26 and S27; HR-FAB-MS found *m/z* 475.2344 [M + H]⁺ (calcd 475.2332 for C₂₆H₃₅O₈). The NMR data are in good agreement with the reported data.²⁹

Terretinin K (13). White amorphous solid; $[\alpha]_D^{22}$ –62.9 (c 1.00, CHCl₃); for UV spectrum, see Figure S7; for ¹H and ¹³C NMR data, see Table S13 and Figures S28 and S29; HR-FAB-MS found *m/z* 477.2485 [M + H]⁺ (calcd 477.2488 for C₂₆H₃₇O₈).

Terretinin L (14). White amorphous solid; $[\alpha]_D^{22}$ +50.5 (c 0.16, CHCl₃); for UV spectrum, see Figure S7; for ¹H and ¹³C NMR data, see Table S14 and Figures S30 and S31; HR-FAB-MS found *m/z* 445.2604 [M + H]⁺ (calcd 445.2590 for C₂₆H₃₇O₆).

Terretinin C (2). White solid; $[\alpha]_D^{22}$ -60.4 (c 1.00, CHCl_3); for UV spectrum, see Figure S7; for ^1H and ^{13}C NMR data, see Table S4 and Figures S10 and S11; HR-FAB-MS found m/z 431.2085 $[\text{M} + \text{H}]^+$ (calcd 431.2070 for $\text{C}_{24}\text{H}_{31}\text{O}_7$). The NMR data are in good agreement with the reported data,^{24,29} but are slightly revised and updated in this study.

Terretinin (1). White solid; $[\alpha]_D^{22}$ -133.1 (c 0.82, CHCl_3); for UV spectrum, see Figure S7; for ^1H and ^{13}C NMR data, see Table S3 and Figures S8 and S9; HR-FAB-MS found m/z 489.2133 $[\text{M} + \text{H}]^+$ (calcd 489.2125 for $\text{C}_{26}\text{H}_{33}\text{O}_9$). The NMR data are in good agreement with the reported data,²⁴ but are slightly revised and updated in this study.

■ ASSOCIATED CONTENT

● Supporting Information

Experimental details, supplementary figures, and spectral data. This material is available free of charge via the Internet at <http://pubs.acs.org>.

■ AUTHOR INFORMATION

Corresponding Author

*abei@mol.f.u-tokyo.ac.jp

Author Contributions

[†]Y.M. and T.I. contributed equally.

Notes

The authors declare no competing financial interest.

■ ACKNOWLEDGMENTS

This paper is dedicated to Professor Shoji Shibata on the occasion of his 100th birthday. We thank Prof. K. Gomi (Tohoku University) and Prof. K. Kitamoto (The University of Tokyo) for kindly providing the expression vectors and the fungal strain. This work was supported by Grants-in-Aid for Scientific Research from the Ministry of Education, Culture, Sports, Science and Technology, Japan.

■ REFERENCES

- (1) Cox, R. J. *Nat. Prod. Rep.* **2014**, *31*, 1405–1424.
- (2) Cochrane, R. V.; Vederas, J. C. *Acc. Chem. Res.* **2014**, *47*, 3148–3161.
- (3) Baunach, M.; Franke, J.; Hertweck, C. *Angew. Chem., Int. Ed.* **2015**, *54*, 2604–2626.
- (4) Chooi, Y.-H.; Hong, Y. J.; Cacho, R. A.; Tantillo, D. J.; Tang, Y. J. *Am. Chem. Soc.* **2013**, *135*, 16805–16808.
- (5) Lin, H.-C.; Tsunematsu, Y.; Dhingra, S.; Xu, W.; Fukutomi, M.; Chooi, Y.-H.; Cane, D. E.; Calvo, A. M.; Watanabe, K.; Tang, Y. J. *Am. Chem. Soc.* **2014**, *136*, 4426–4436.
- (6) Tsunematsu, Y.; Ishikawa, N.; Wakana, D.; Goda, Y.; Noguchi, H.; Moriya, H.; Hotta, K.; Watanabe, K. *Nat. Chem. Biol.* **2013**, *9*, 818–825.
- (7) Hu, Y.; Dietrich, D.; Xu, W.; Patel, A.; Thuss, J. A.; Wang, J.; Yin, W.-B.; Qiao, K.; Houk, K.; Vederas, J. C. *Nat. Chem. Biol.* **2014**, *10*, 552–554.
- (8) Teufel, R.; Miyana, A.; Michaudel, Q.; Stull, F.; Louie, G.; Noel, J. P.; Baran, P. S.; Palfey, B.; Moore, B. S. *Nature* **2013**, *503*, 552–556.
- (9) Matsuda, Y.; Awakawa, T.; Wakimoto, T.; Abe, I. *J. Am. Chem. Soc.* **2013**, *135*, 10962–10965.
- (10) Matsuda, Y.; Wakimoto, T.; Mori, T.; Awakawa, T.; Abe, I. *J. Am. Chem. Soc.* **2014**, *136*, 15326–15336.
- (11) Ishikawa, N.; Tanaka, H.; Koyama, F.; Noguchi, H.; Wang, C. C.; Hotta, K.; Watanabe, K. *Angew. Chem., Int. Ed.* **2014**, *53*, 12880–12884.
- (12) Itoh, T.; Tokunaga, K.; Matsuda, Y.; Fujii, I.; Abe, I.; Ebizuka, Y.; Kushiro, T. *Nat. Chem.* **2010**, *2*, 858–864.
- (13) Takahashi, S.; Toyoda, A.; Sekiyama, Y.; Takagi, H.; Nogawa, T.; Uramoto, M.; Suzuki, R.; Koshino, H.; Kumano, T.; Panthee, S.;

Dairi, T.; Ishikawa, J.; Ikeda, H.; Sakaki, Y.; Osada, H. *Nat. Chem. Biol.* **2011**, *7*, 461–468.

(14) Sun, P.; Zhao, Q.; Yu, F.; Zhang, H.; Wu, Z.; Wang, Y.; Wang, Y.; Zhang, Q.; Liu, W. *J. Am. Chem. Soc.* **2013**, *135*, 1540–1548.

(15) Bretschneider, T.; Heim, J. B.; Heine, D.; Winkler, R.; Busch, B.; Kusebauch, B.; Stehle, T.; Zocher, G.; Hertweck, C. *Nature* **2013**, *502*, 124–128.

(16) Hashimoto, T.; Hashimoto, J.; Teruya, K.; Hirano, T.; Shin-Ya, K.; Ikeda, H.; Liu, H.-w.; Nishiyama, M.; Kuzuyama, T. *J. Am. Chem. Soc.* **2015**, *137*, 572–575.

(17) Springer, J. P.; Dorner, J. W.; Cole, R. J.; Cox, R. H. *J. Org. Chem.* **1979**, *44*, 4852–4854.

(18) McIntyre, C. R.; Simpson, T. J. *J. Chem. Soc., Chem. Commun.* **1981**, *20*, 1043–1044.

(19) McIntyre, C. R.; Simpson, T. J.; Stenzel, D. J.; Bartlett, A. J.; O'Brien, E.; Holker, J. S. E. *J. Chem. Soc., Chem. Commun.* **1982**, 781–782.

(20) McIntyre, C. R.; Scott, F. E.; Simpson, T. J.; Trimble, L. A.; Vederas, J. C. *Tetrahedron* **1989**, *45*, 2307–2321.

(21) Geris, R.; Simpson, T. J. *Nat. Prod. Rep.* **2009**, *26*, 1063–1094.

(22) Itoh, T.; Tokunaga, K.; Radhakrishnan, E. K.; Fujii, I.; Abe, I.; Ebizuka, Y.; Kushiro, T. *ChemBioChem* **2012**, *13*, 1132–1135.

(23) Matsuda, Y.; Awakawa, T.; Itoh, T.; Wakimoto, T.; Kushiro, T.; Fujii, I.; Ebizuka, Y.; Abe, I. *ChemBioChem* **2012**, *13*, 1738–1741.

(24) Guo, C.-J.; Knox, B. P.; Chiang, Y.-M.; Lo, H.-C.; Sanchez, J. F.; Lee, K.-H.; Oakley, B. R.; Bruno, K. S.; Wang, C. C. *Org. Lett.* **2012**, *14*, 5684–5687.

(25) Lo, H.-C.; Entwistle, R.; Guo, C.-J.; Ahuja, M.; Szweczyk, E.; Hung, J.-H.; Chiang, Y.-M.; Oakley, B.; Wang, C. C. *J. Am. Chem. Soc.* **2012**, *134*, 4709–4720.

(26) Jin, F. J.; Maruyama, J.; Juvvadi, P. R.; Arioka, M.; Kitamoto, K. *FEMS Microbiol. Lett.* **2004**, *239*, 79–85.

(27) Matsuda, Y.; Awakawa, T.; Abe, I. *Tetrahedron* **2013**, *69*, 8199–8204.

(28) Barriuso, J.; Nguyen, D. T.; Li, J. W.-H.; Roberts, J. N.; MacNevin, G.; Chaytor, J. L.; Marcus, S. L.; Vederas, J. C.; Ro, D.-K. *J. Am. Chem. Soc.* **2011**, *133*, 8078–8081.

(29) Li, G.-Y.; Li, B.-G.; Yang, T.; Yin, J.-H.; Qi, H.-Y.; Liu, G.-Y.; Zhang, G.-L. *J. Nat. Prod.* **2005**, *68*, 1243–1246.

(30) López-Gresa, M. P.; Cabedo, N.; González-Mas, M. C.; Ciavatta, M. L.; Avila, C.; Primo, J. J. *Nat. Prod.* **2009**, *72*, 1348–1351.

(31) Liu, X.-H.; Miao, F.-P.; Qiao, M.-F.; Cichewicz, R. H.; Ji, N.-Y. *RSC Adv.* **2013**, *3*, 588–595.

(32) Kelley, L. A.; Sternberg, M. J. *Nat. Protoc.* **2009**, *4*, 363–371.

(33) Cho, H.-S.; Ha, N.-C.; Choi, G.; Kim, H.-J.; Lee, D.; Oh, K. S.; Kim, K. S.; Lee, W.; Choi, K. Y.; Oh, B.-H. *J. Biol. Chem.* **1999**, *274*, 32863–32868.

(34) Arand, M.; Hallberg, B. M.; Zou, J.; Bergfors, T.; Oesch, F.; van der Werf, M. J.; de Bont, J. A.; Jones, T. A.; Mowbray, S. L. *EMBO J.* **2003**, *22*, 2583–2592.

(35) Sultana, A.; Kallio, P.; Jansson, A.; Wang, J. S.; Niemi, J.; Mäntsälä, P.; Schneider, G. *EMBO J.* **2004**, *23*, 1911–1921.

(36) Minami, A.; Ose, T.; Sato, K.; Oikawa, A.; Kuroki, K.; Maenaka, K.; Oguri, H.; Oikawa, H. *ACS Chem. Biol.* **2013**, *9*, 562–569.

(37) Whittingham, J. L.; Turkenburg, J. P.; Verma, C. S.; Walsh, M. A.; Grogan, G. *J. Biol. Chem.* **2003**, *278*, 1744–1750.

(38) Yang, Y.; Ko, T. P.; Liu, L.; Li, J.; Huang, C. H.; Chan, H. C.; Ren, F.; Jia, D.; Wang, A. H. J.; Guo, R. T.; Chen, J.; Du, G.-C. *ChemBioChem* **2014**, *15*, 1882–1886.

(39) Fujii, T.; Yamaoka, H.; Gomi, K.; Kitamoto, K.; Kumagai, C. *Biosci. Biotechnol. Biochem.* **1995**, *59*, 1869–1874.

(40) Yamada, O.; Na Nan, S.; Akao, T.; Tominaga, M.; Watanabe, H.; Satoh, T.; Enei, H.; Akita, O. *J. Biosci. Bioeng.* **2003**, *95*, 82–88.

(41) Yamada, O.; Lee, B. R.; Gomi, K.; Iimura, Y. *J. Biosci. Bioeng.* **1999**, *87*, 424–429.

(42) Jin, F.; Maruyama, J.; Juvvadi, P.; Arioka, M.; Kitamoto, K. *Biosci. Biotechnol. Biochem.* **2004**, *68*, 656–662.

(43) Gomi, K.; Iimura, Y.; Hara, S. *Agric. Biol. Chem.* **1987**, *51*, 2549–2555.